

# SINBAD mobile bed experiment – Hydrodynamics and Sand Transport over a mobile sandy bed.

## Description processed dataset

Joep van der Zanden, Dominic A. van der A, Iván Cáceres, Guillaume Fromant,  
David Hurther, Tom O'Donoghue, and Jan S. Ribberink

## General remarks

### Introduction

The present data have been collected during a mobile-bed experiment in the CIEM wave flume at UPC, Barcelona, during a two-month campaign (May-June 2014) as part of the STW/EPSRC-funded SINBAD project (University of Twente, University of Aberdeen, University of Liverpool, 2012-2016). The experiment focused on extending insights in sand transport processes under an energetic, large-scale breaking waves. Measurements have been obtained of water surface, water velocity, turbulence, sand concentration, sand fluxes, bed profile evolution, and sand transport rates.

Results have been presented in the following peer-reviewed journal papers:

- van der Zanden, J., D. A. van der A, D. Hurther, I. Cáceres, T. O'Donoghue, and J. S. Ribberink (2016), *Near-bed hydrodynamics and turbulence below a large-scale plunging breaking wave over a mobile barred bed profile*, J.Geophys. Res. Oceans: 121, 6482–6506, doi: 10.1002/2016JC011909.
- van der Zanden, J., D. A. van der A, D. Hurther, I. Cáceres, T. O'Donoghue, and J. S. Ribberink (2017), *Suspended sediment transport around a large-scale laboratory breaker bar*, Coastal Engineering, 125, 51-69, doi: 10.1016/j.coastaleng.2017.03.007
- van der Zanden, J., D. A. van der A, D. Hurther, I. Cáceres, T. O'Donoghue, S. J. M. H. Hulscher and J. S. Ribberink (2017). *Bedload and suspended load contributions to breaker bar morphodynamics*. Coastal Engineering, 129, 74-92, doi: 10.1016/j.coastaleng.2017.09.005
- Fromant, G., Hurther, D., van der Zanden, J., van der A, D. A., Cáceres, I., O'Donoghue, T. and J. S. Ribberink (2018). *Wave boundary layer hydrodynamics and sheet flow properties under large-scale plunging-type breaking waves*. Journal of Geophysical Research Oceans, in press, doi: 10.1029/2018JC014406

Preliminary versions of the vdZ *ea* papers are found in Chapters 2-4 in the PhD thesis of Joep van der Zanden (2016; *Sand Transport Processes in the Surf and Swash Zones*). The present data correspond to the journal papers version, i.e. the most recent and final results.

### About the experiments

Regular waves ( $T = 4\text{s}$ ;  $H_0 = 0.85\text{ m}$ ) were generated, resulting in plunging breaking over a mobile test section (medium sand,  $D_{50} = 0.25\text{ mm}$ ). The experiment departed from an initially flat horizontal test

section, allowing the bed profile to develop during a start-up stage of 105 minutes (7 runs of 15 min.). The accordingly obtained breaker bar + trough configuration was used as a template ('reference bed profile,  $t = 0$ '). The experiment consisted of an additional 90 min. of wave action (6 runs of 15 min.). After each experimental run, the mobile frame was lowered/raised to maintain an approximately constant relative position with respect to the local bed level at the start of each run.

The experiment was repeated 12 times, on each repeat departing from the same reference bed profile. At each experimental repeat, the mobile measuring frame (containing most instruments) was positioned to a new cross-shore location. This procedure yielded a total 72 runs, with measurements at 12 cross-shore positions for six 15-min. stages of bar development. Appendix A shows an overview with the cross-shore locations of the mobile measuring frame for all 72 experimental runs.

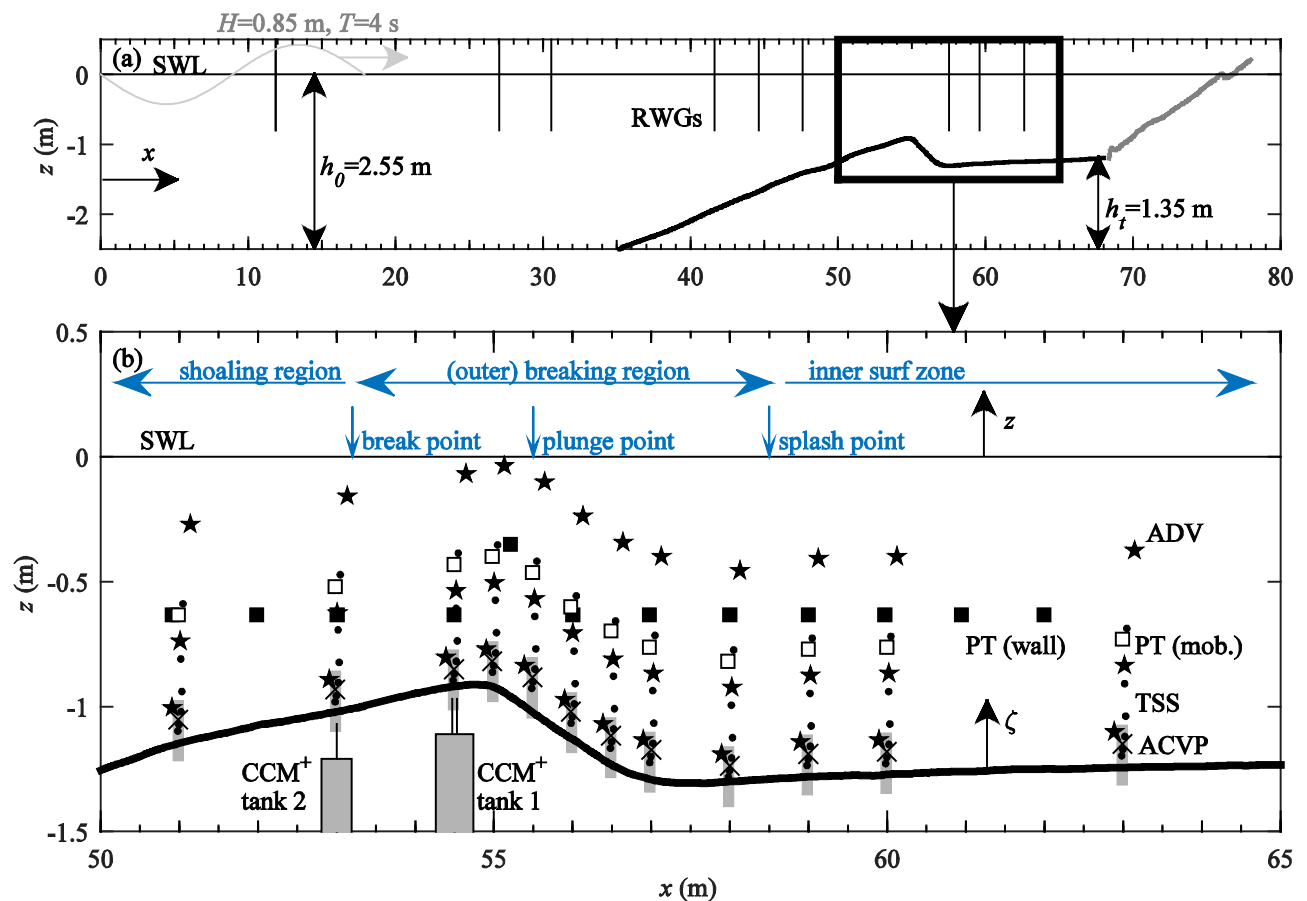


Figure 1. Positions of instruments at start of experiment.

Cross-shore coordinates  $x$  are defined positively towards the beach with  $x = 0$  at the wave paddle in lowest position. The vertical coordinate  $z$  is defined positively upward from the water level. Vertical coordinate  $\zeta$  ('zeta' in data files) is defined positively upward from the local bed level. Figure 1 shows the positions of all instruments at the start of each experiment. More information is found in the journal papers.

### Folder organization:

- 0\_General
- 1\_Datareports, notes
- 2\_Publications
- 3\_Processed\_data
- 4\_Raw\_data
- 5\_Photos
- 6\_Other

0\_General: PDF with data description.

1\_Datareports: Data report and log book.

2\_Publications: Peer-reviewed publications corresponding to this data-set.

3\_Processes\_data: Processed, phase-averaged data files organized per instrument.

4\_RAW\_data: Raw data.

5\_Photos: Photos and videos of the experiment.

6\_Other: BSc and MSc reports connected to this experiment.

### Format

All data are stored as .txt files (tab-delimited). Instants with no valid data record (e.g. measurement above water surface/outliers) are listed as -999.

### Raw data files

To limit the size of the dataset, the repository focuses on the cleaned and processed data. Generally this means phase-averaged or time-averaged results. The raw data and time series are available upon request.

### Contact information

For questions/remarks, please get in touch with dr. Joep van der Zanden ([j.vanderzanden@utwente.nl](mailto:j.vanderzanden@utwente.nl), [vanderzandenjoep@gmail.com](mailto:vanderzandenjoep@gmail.com)).

### Referencing

When using the dataset, please refer to the peer-reviewed journal papers and not to the repository.

## 1\_Datareports

The data storage report (*Data\_report\_SINBAD\_II.PDF*) contains extensive descriptions of the measurement procedures, the applied instrumentation, and storage of the raw data files. Note that no data report of the processed data is available; the peer-reviewed journal papers are believed to provide all information required to work with the processed data.

Two log files (.xls) were kept. These log files are to be used in combination with the data report for information about each experimental run. *SINBAD\_MBLOGBOOK\_final.xls* was kept by the SINBAD team and contains information about the mobile-frame instrumentation, including positions, and additional remarks for each experimental run. *sinbad\_II\_CONTROL.xls* was kept by the CIEM staff, and contains information especially about instrumentation connected to the CIEM acquisition system.

## 2\_Publications

Publications connected to this dataset.

## 3\_Processed data

Each folder contains the organized processed data. Data are stored as .txt files, including metadata in the header rows.

- 01\_Bed profiles
- 02\_Water surface level
- 03\_Pressure
- 04\_Velocity ADV
- 05\_Velocity ACVP
- 06\_Turbulence ADV
- 07\_Turbulence ACVP
- 08\_Concentration TSS
- 09\_Concentration ACVP
- 10\_Fluxes ACVP
- 11\_Grain size
- 12\_Sheet flow CCM
- 13\_SRP bed scans
- 14\_Transport rates
- 15\_Sheet flow ACVP

### 01\_Bed profiles

*Pmean.txt* contains the ensemble-mean profile measurements at  $t = 0$  min (initial profile), 30 min, 60 min, and 90 min (final profile), respectively (columns 2-5). Column 1 is the  $x$  location. Values were obtained by averaging acoustic profile measurements over 11 experimental repeats (data from one experimental repeat were discarded).

*Pfix.txt* is the profile of the fixed beach, measured with a wheel profiler.

### All\_profiles folder

This subfolder contains all processed acoustic bed profile measurements. Outliers were removed and linearly interpolated. The three columns denote the  $x$  location (in m) and the bed level  $z$  (in m) as measured using acoustic sensors 1 and 2, respectively. Use the data storage report to see the date/time/run for each profile measurement.

### 02 Water surface level

Water surface levels were measured with resistive wave gauges (RWGs), deployed from the flume's side-walls, mainly along the offshore slope of the bar.

Additional water surface level estimates were derived from pressure measurements, by pressure transducers (PTs) deployed from the flume's side-walls and from the mobile measuring frame. The full time series of these pressure measurements were converted to water surface level following the spectral-based approach of Guza and Thornton (1980). Note that the applied approach is based on linear wave theory and could only be applied up to frequencies of 0.33 Hz. This means that for strongly asymmetric waves, the PT-derived water surface level has a lower steepness (skewness/asymmetry) and wave height than the actual wave height.

At a total of 34 cross-shore locations measurements are available (10\*RWG, 12\*PT wall, 12\*PT frame).

### Phase-averaged

Contains phase-averaged water surface level measurements by RWGs and PTs. Data are sorted for six stages of bar development. RWG and PT (wall) values were measured during the very first run. PT (mobile frame) measurements were measured during the first run of each of 12 experimental repeats.

### Wave-averaged

Time-averaged water surface level statistics at 34 locations:

- Wave height  $H$
- Maximum and minimum phase-averaged water surface level  $\langle \eta \rangle_{\max}$ ,  $\langle \eta \rangle_{\min}$
- Time-averaged water surface level (set-up/set-down)
- Root-mean-square water surface level
- Instrument identifier: (1) = RWG; (2) = wall-deployed PT; (3) = mobile frame PT.

NB time series are found in the folder '4\_RawData'.

### 03 Pressure measurements

Phase-averaged measurements of the dynamic pressure head in m (i.e. hydrostatic contribution is subtracted). At 12 ( $x,z$ ) positions using PTs deployed from wall, and at another 12 ( $x, z$ ) positions using PTs deployed from mobile measuring frame.

### 04 Velocity ADV

Date were despiked and cleaned based on signal to noise ratio and correlation values, see van der Zanden *et al.* (2016, JGR). Outliers were removed and not interpolated; data were then phase-averaged.

Note that time series of ADV velocities are available in the RawData folder.

### Phase-averaged velocity

18 files denote phase-averaged cross-shore horizontal velocity  $u$ , horizontal transverse (i.e. longshore) velocity  $v$ , and vertical velocity  $w$ , for six stages of bar development. Each file contains three header rows ( $x$ ,  $z$  and  $\zeta$  location); the first column is the normalized time  $t/T$  and columns 2 to 37 give the measured velocities.

### Time-averaged velocity statistics

For each ensemble-mean (i.e. 36  $x,z$  locations), the following velocity statistics were calculated:

- $u\_bar$  = time-averaged horizontal velocity  $\bar{u}$  (note, averaged over 'wet period', so using nanmean!)
- $urms$  = root-mean-square orbital velocity
- $umax, umin$  = maximum and minimum phase-averaged horizontal velocity  $\langle u \rangle_{max}$ ,  $\langle u \rangle_{min}$
- $u\_Sk, u\_Asy$  = horizontal  $u$  orbital velocity skewness and asymmetry, calculated as  

$$u\_Sk = skewness(uorb);$$

$$u\_Asy = -mean(imag(hilbert(uorb)).^3) ./ std(uorb).^3;$$
- $wbar$  = time-averaged vertical velocity
- $wrms$  = root-mean-square vertical velocity
- $vbar$  = time-averaged transverse (longshore) velocity

### 05\_Velocity ACVP

Phase- and time-averaged ACVP data are stored per run. All velocities are given in non-rotated horizontal, vertical ( $u, w$ ) and in rotated bed-parallel, bed-normal ( $u_R, w_R$ ) form.

ACVP\_stats.txt provides reference information for each run: the  $x$  location; stage of bar development within the experiment (1 = 0-15 min; 6 = 75-90 min.); crest-phase periodic velocity overshoot elevation  $\delta$  (m), proxy for the WBL thickness; the angle used for rotating the velocity; the local water depth (m).

NB the rotation angle was found through minimizing the bed-normal periodic velocities near the bed. It is generally close to the bed slope obtained from the bed profile measurements, but local offsets occur.

### Phase-averaged measurements

Velocity subfolders and files store the horizontal and vertical velocity. Annex '\_rot' in the filename indicates velocities have been rotated. In each file, row 1 is the normalized time  $t/T$ ; column 1 is the vertical elevation  $\zeta$  (m); the remainder of the file presents the phase-averaged velocity. The bed level files store the intra-wave bed level measured by ACVP.

### Time-averaged measurements

Distinction is again made between measurements in the  $x, z$  plane and in the rotated plane. Each file 'velstats\_run\*x\*.txt' contains near-bed vertical profiles of the same velocity statistics as given for the ADV (See 04\_Velocity ADV for an overview of the variables)

### 06\_Turbulence ADV

A Reynolds decomposition was applied to calculate  $u'_{rms}$ ,  $v'_{rms}$ ,  $w'_{rms}$  and the turbulent Reynolds stress ( $-u'w'$ ). Turbulent kinetic energy (TKE) is calculated as  $0.5*(u'^2 + v'^2 + w'^2)$ .

#### Phase-averaged

Phase-averaged variables  $u'_{rms}$ ,  $v'_{rms}$ ,  $w'_{rms}$ , the turbulent Reynolds stress ( $-u'w'$ ) and the turbulent kinetic energy (TKE) are each stored in separate files, for all six stages of bed profile development. Each file contains three header rows (x, z and  $\zeta$  location); the first column is the normalized time  $t/T$  and columns 2 to 37 give the measured turbulent quantities.

#### Time-averaged

The time-averaged file contains the same turbulence statistics, i.e.:

- $\bar{u}'$ ,  $\bar{v}'$ ,  $\bar{w}'$
- $Re = -\bar{u}'\bar{w}'$
- TKE ( $\bar{k}$ )

at 36 locations (12 cross-shore, 3 vertical).

### 07\_Turbulence ACVP

ACVP turbulence intensities were based on *rotated* velocities, i.e.  $\langle u_{R,rms} \rangle$  and  $\langle w_{R,rms} \rangle$ . For convenience the subscript 'R' is omitted in the files. Note that (acoustic) noise was removed from the turbulent measurements by applying Garbini's (1982) cross-correlation method; see Appendix A in van der Zanden *et al.* (2016). Note further that close to the bed, where eddies are small, due to the relative coarse sampling volume compared to the length scales of the eddies, turbulent fluctuations are not accurately resolved by the ACVP and (especially the vertical) turbulence intensities are underestimated (see also Appendix A in vdZ (2016)). TKE is calculated as  $\langle k \rangle = 1.39*0.5*(u_{R,rms}^2 + w_{R,rms}^2)$ .

Note that the folders contain a few 'empty' files; for these runs the turbulence data were discarded because not enough wave cycles were sampled for an accurate measurement of the turbulence intensity. Reasons for this were particularly the rapid erosion/accretion rate at some cross-shore locations.

#### Phase-averaged

Similar to data in '05\_Velocity ACVP', phase-averaged data are stored per run and per variable, with

- $upr_{rms} = \langle u_{R,rms} \rangle$
- $wpr_{rms} = \langle w_{R,rms} \rangle$
- TKE =  $\langle k \rangle$

In each file, row 1 is the normalized time  $t/T$ ; column 1 is the vertical elevation  $\zeta$  (m); the remainder of the file presents the phase-averaged data.

#### Time-averaged

The files contain the vertical profiles of time-averaged  $u_{R,rms}$ ,  $w_{R,rms}$ , and TKE per run.

### 08 Concentration TSS

Each file contains time-averaged concentrations measured with the transverse suction system at six elevations; column 1 = x location; column 2 =  $\zeta$  elevation; column 3 = concentration in  $\text{kg/m}^3$ .

Suction pumps were started at 1 minute following the start of each run and stopped after directly following the last wave. Note that for considerable runs the suction system blocked because the bed level increased rapidly. These data were discarded (-999 values in data file).

The  $\zeta$  level in the file is the time-averaged (i.e. averaged over the acquisition period) vertical elevation with respect to the local bed level during the run. I.e., this vertical elevation was corrected for local bed evolution using continuous bed level measurements by the ACVP.

### 09 Concentration ACVP

ACVP concentrations are obtained by inverting the acoustic backscatter intensity, as explained in van der Zanden *et al.* (2017a). The inversion is considered accurate for  $\zeta > 0.005$  m; the concentration measurements at lower elevations are discarded. Data are organized similar to data in '05\_Velocity ACVP', i.e. per run.

In each phase-averaged data file, row 1 is the normalized time  $t/T$ ; column 1 is the vertical elevation  $\zeta$  (m); the remainder of the file presents the phase-averaged sediment concentration in  $\text{kg/m}^3$ . The time-averaged data files contain the vertical profiles of time-averaged concentration.

### 10 Fluxes ACVP

Fluxes are found as the product of collocated velocity and concentration measurements. Note that the ACVP provides all flux components, i.e. the total flux  $\overline{uC}$  can be decomposed into a current-related component  $\overline{u\bar{C}}$ , a wave-related component  $\overline{\tilde{u}\tilde{C}}$ , and a turbulent component  $\overline{u'C'}$ . Distinction is made between horizontal fluxes  $uC$  and bed-parallel fluxes  $u_R C$ .

NB. Vertical/bed-normal fluxes are not provided for two reasons: (1) the vertical turbulent flux was not accurately resolved over the complete profile due to ACVP measurement constraints (see Appendix A in van der Zanden *et al.*, 2016); (2) the vertical fluxes are dominated by the undertow (i.e. the vertical component of bed-parallel velocity) while the bed-normal fluxes are very sensitive to the applied rotation angle.

#### Phase-averaged

Phase-averaged total sediment flux in horizontal direction  $\langle uC \rangle$  ('uC\_acvp\_run\*xx\*.txt') and in bed-parallel direction  $\langle u_R C \rangle$  ('urotC\_acvp\_run\*xx\*.txt'). Note that the files provide the total flux, i.e. all three flux components. The individual flux components can be inferred from the data, i.e.  $\langle \tilde{u}\tilde{C} \rangle = \langle uC \rangle - \overline{u\bar{C}}$ , and  $\langle u'C' \rangle = \langle uC \rangle - \langle u \rangle \langle C \rangle$  (with  $\langle u \rangle$  and  $\langle C \rangle$  found in folders '05\_Velocity ACVP' and '09\_Concentration ACVP').

#### Time-averaged

Per run, vertical profiles are given of time-averaged:

- Concentration  $C$  ( $\text{kg/m}^3$ )
- The total flux  $\overline{uC}$ , current-related flux  $\overline{u\bar{C}}$ , wave-related flux  $\overline{\tilde{u}\tilde{C}}$ , and turbulent flux  $\overline{u'C'}$  (units:  $\text{kg/m}^2\text{s}$ ) in horizontal direction.
- The same flux components in bed-parallel direction.

### 11 Grain size

Grain size distributions were analyzed using a Beckhoff Laser Diffraction particle sizer. The particle sizer splits each sediment sample in three, and measures the grain size characteristics for each of the three sub-samples. The present folder contains only the  $D_{10}$ ,  $D_{50}$  and  $D_{90}$  values. Note that the full grain size distribution was measured, and more detailed data are found in the Raw Data folder.

Note that grain sizes by the laser-diffraction system are somewhat higher than values provided by independent sieving tests at UPC (see data storage report for grain size specifications obtained through sieving).

### Bed samples

Bed samples were at each cross-shore location taken at three alongshore positions by scraping off the top few cm of sediment. These three samples were then combined into one mixed sample for each cross-shore location. For locations with bed forms, the top layer of a complete bed form (in cross-shore direction) was scraped off.

Bed samples were taken at three stages of the experiment:

- At the very beginning of the experiment, i.e. with profile consisting of a horizontal test section (1\_GrainSize\_initialprofile.txt).
- After the initial 105-min. start-up stage, i.e. corresponding to the reference bed level: (2\_GrainSize\_refprofile.txt).
- At the end of the last run i.e. corresponding to the final bed level: (3\_GrainSize\_finalprofile.txt)

Each file contains the  $x$  position, the  $D_{10}$ ,  $D_{50}$  and  $D_{90}$  (in  $\mu\text{m}$ ). Values are means over three measurements by the laser-diffraction system.

### Suspension samples

For the suspension samples, some samples corresponding to the same nozzle (i.e. elevation  $\zeta$ ) were merged to ensure sufficient sediment for a reliable measurement (see van der Zanden *et al.*, 2017a). E.g. at  $x = 51.0$  m, for each nozzle a mixed sample was taken over multiple runs. Hence, data for  $t=0-15$  min. are the same as  $t = 15-30$  min. for this location.

Each file contains the  $x$  location,  $\zeta$  elevation, TSS concentration,  $D_{10}$ ,  $D_{50}$  and  $D_{90}$ .

### 12 Sheet flow CCM+

Sheet flow layer dynamics were measured with CCM<sup>+</sup> at two cross-shore locations at the breaker bar. Tank 1 (large tank, 3 probes) was at  $x = 54.5$  m. Tank 2 (small tank, 1 probe) was positioned somewhat further offshore at  $x = 53.0$  m.

### Concentrations

C\_tk1 and C\_tk2 contain matrices with ensemble-averaged concentrations. In each file, row 1 is the time  $t/T$ ; column 1 is the vertical elevation  $\zeta$ ; the remainder are the volumetric concentrations (in  $\text{m}^3/\text{m}^3$ ).

### Sheet flow layer thickness

Time-varying sheet flow layer thickness ( $\delta_s$ ), erosion depth ( $\delta_e$ ) and sheet flow layer top. Values found by fitting curve O'Donoghue and Wright (2004) through measurements, as detailed in van der Zanden *et al.* (2017b).

### Particle velocity

Phase-averaged particle velocities based on cross-correlation between probe 1 and 2, CCM+ tank 1 only ( $x=54.5$  m). In each file, column 1 is the time  $t/T$ ; column 2 is the vertical elevation  $\zeta$ ; column 3 is the volumetric sediment concentration (in  $m^3/m^3$ ); column 4 is the grain velocity (in m/s).

### 13 SRP bed scans

Continuous sand ripple scan measurements were made during each run. The SRP data were not used for an in-depth analysis. The raw SRP scans and a processing routine to transform the acoustic backscatter intensity to the x-y plane are available in the Raw Data folder.

### 14 Transport rates

qtot.txt contains the total transport rates, obtained from bed profile measurements through solving a mass balance equation. Column 1 marks  $x$  location; columns 2-4 the transport rates [ $m^2/s$ ] for three time intervals (0-30 min, 30-60 min, 60-90 min), i.e. mean  $q_{tot}$  rates over 11 experimental repeats; columns 5-7 present the standard deviation of the mean for the corresponding ensemble-mean  $q_{t=t}$  rates.

At the 12 cross-shore mobile-frame measurement locations, the transport rate is decomposed into various components:

- $q_{sc}$  is the depth-integrated current-related transport  $q_{sc} = \int_{z_a}^{\eta_{crest}} \overline{u\bar{c}}d\zeta$ , where  $z_a = 0.005$  m is the elevation marking the intersect between bedload ( $\zeta < z_a$ ) and suspended load ( $\zeta > z_a$ );  $\eta_{crest}$  is the maximum crest-phase water surface level.
- $q_{sw}$  is the depth-integrated wave-related transport over the near-bed elevations sampled with ACVP (about 0.10 m). Note that this flux is largely restricted to the wave bottom boundary layer.  
 $q_{sw} = \int_{z_a}^{0.10} \overline{u\bar{c}}d\zeta$ .
- $q_{bed}$  is the bedload transport rate, obtained indirectly by subtracting the suspended load transport from the total transport rate, i.e.  $q_{bed}(x) = q_{tot}(x) - q_{sc}(x) - q_{sw}(x)$
- $q_{s\_wbl}$  is the suspended load transport inside the WBL, i.e.  $q_{s\_wbl} = \int_{z_a}^{\delta} \overline{u\bar{c}}d\zeta$ , where  $\delta$  marks the crest-phase wave bottom boundary layer overshoot elevation.
- $q_{s\_outer}$  is the suspended load transport at outer flow above the WBL, i.e.  $q_{s\_outer} = \int_{\delta}^{\eta_{crest}} \overline{u\bar{c}}d\zeta$

Each file shows the accordingly obtained transport rates at 12 locations [ $*10^6$   $m^2/s$ ], for all six stages of bed profile development. Note that some estimates are subjected to considerable scatter; averaging over the full experiment (six runs per location) may be advised.

## 15. Sheet Flow ACVP data

This folder contains the ACVP data covering the sheet flow layer in the shoaling and outer surf zone. Each subfolder is named after the corresponding run number and contains three .txt files. The runs gathered here only cover 5 cross-shore locations between  $x = 51$  m and  $x = 55.5$  m, thus covering the shoaling and outer surf zone. The content of the .txt (tab delimited ascii format) files is as follows:

- "runX\_sheet\_flow\_interfaces.txt" : contains 7 lines in total, respectively corresponding to the 1/ the run number, 2/ the cross-shore position, 3/ the intrawave phase vector  $t/T$ , proportional to the wave period, 4/ the vertical reference  $z$  (relative to the no-flow bed level), 5/ the intrawave upper sheet flow layer interface  $\delta_u$ , 6/ the intrawave erosion depth  $\delta_e$ , and 7/ the intrawave sheet flow layer thickness  $\delta_s$ .  $\delta_e$  results from the bed detection using the ACVP intensity raw file for each wave, further averaged out over all waves.
- "runX\_sheet\_flow\_conc\_all\_waves.txt": contains the bed-referenced (relative to the no-flow bed level) concentration time series (2D-matrix). The  $z$  vector is to be used for vertical reference.
- "runX\_sheet\_flow\_velocity\_all\_waves.txt": contains the bed-referenced (relative to the no-flow bed level) velocity time series (2D-matrix). The  $z$  vector is to be used for vertical reference.

A (commented) Matlab file is provided in the same folder, enabling to read the .txt files and storing the target values in the workspace. Note that wave separation is also applied on the concentration and velocity time series, resulting in the creation of a 3D matrix (wave number \* phase number \* vertical cell number) from which phase-averaged concentration and velocity can be computed. The  $t/T$  vector stored in the "\*\_interfaces.txt" file is to be used for the phase number reference.

The methodology for flux decomposition is presented in 10\_Fluxes ACVP. The same methodology has been used to estimate the mean, orbital and turbulent contribution of the flux relative to the total flux.

## 4\_Raw data

The raw measurements of water surface, velocity, and sand concentration are available upon request by e-mail.

### Grain size data

The folder contains the output of the Beckman LS13320 Laser-Diffraction Particle Sizer. For each sediment sample, three measurements of the grain size distributions were done. Note that some suction samples were merged to have sufficient sediment for the measurement.

Suspended sediment measurements are stored as follows:

- 'r \*x\* n \*y\* \_01\_ \*z\*.\$ls' : measurements for run \*x\*, nozzle \*y\*. Index \*z\* is used for referencing.
- 'r \*x\* r \*x+1\* n \*y\* \_01\_ \*z\*.\$ls' : measurement for combined sample runs \*x\* and run \*x+1\*
- 'r \*x\* tm \*x+i\* n \*y\* \_01\_ \*z\*.\$ls' : measurement for combined sample runs \*x\* to run \*x+i\*

NB nozzle 1 is the nozzle closest to the bed; nozzle 6 is the highest nozzle.

Bed samples were taken at three stages:

- At the very beginning of the experiment, i.e. with profile consisting of a horizontal test section: 'fbed1-\*x\*....\$ls', where \*x\* denotes an identifier for the measurement location as per below.
- After the initial 105-min. start-up stage, i.e. corresponding to the reference bed level: 'loc\*x\*init....\$ls', where \*x\* denotes an identifier for the measurement location as per below.
- At the end of the last run i.e. corresponding to the final bed level: 'bedend\*x\* ....\$ls', where \*x\* denotes an identifier for the measurement location as per below.

Table: *X* location for each \*x\* measurement identifier.

File \ *x* ID.	1	2	3	4	5	6	7	8	9	10	11	12
Fbed1-*x*	51	53	54	54.5	55	55.5	56	57	58	60	63	-
loc*x*init	51	53	54	54.5	55	55.5	56	57	58	60	63	
bedend	51	53	54.5	55	55.5	56	56.5	57	58	59	60	63

NB the measurement locations for various stages of bar development are not exactly the same (see Table above). The reason for this is that the mobile-frame measurement locations visited during the experiment were slightly different than scheduled prior to the experiment. The final bed sample measurements (12 locations) correspond to the 12 measurement locations sampled with the mobile frame instrumentation.

### Bed scans using Sand Rippler Profiler (SRP)

Continuous SRP scans were made during each run. The raw data are available upon request by e-mail. The folder contains figures of the (raw) bed scans.

## 5\_Photos

Photos and videos of the experiment.

## 6\_Other

The folder contains the following BSc and MSc graduation projects involving the present experimental data:

- BSc thesis Mick Poppe: *Suspended sediments under plunging waves*
- MSc thesis Abe Esselink: *Measuring turbulence along a breaker bar*
- MSc thesis Bram Schnitzler: *Modeling sand transport under breaking waves*

These graduation projects were conducted at the University of Twente during the SINBAD project. **Note that preliminary versions of the processed data were used during these graduation projects.**

## References

### SINBAD mobile bed experiment:

- Fromant, G., Hurther, D., van der Zanden, J., van der A, D. A., Cáceres, I., O'Donoghue, T. and J. S. Ribberink (2018). *Wave boundary layer hydrodynamics and sheet flow properties under large-scale plunging-type breaking waves*. *Journal of Geophysical Research Oceans*, in press, <http://dx.doi.org/10.1029/2018JC014406>
- van der Zanden, J., D. A. van der A, D. Hurther, I. Cáceres, T. O'Donoghue, and J. S. Ribberink (2016), *Near-bed hydrodynamics and turbulence below a large-scale plunging breaking wave over a mobile barred bed profile*, *J.Geophys. Res. Oceans*: 121, 6482–6506, <http://dx.doi.org/10.1002/2016JC011909>.
- van der Zanden, J., D. A. van der A, D. Hurther, I. Cáceres, T. O'Donoghue, and J. S. Ribberink (2017a), *Suspended sediment transport around a large-scale laboratory breaker bar*, *Coastal Engineering*, 125, 51-69, <http://dx.doi.org/10.1016/j.coastaleng.2017.03.007>
- van der Zanden, J., D. A. van der A, D. Hurther, I. Cáceres, T. O'Donoghue, S. J. M. H. Hulscher and J. S. Ribberink (2017b). *Bedload and suspended load contributions to breaker bar morphodynamics*. *Coastal Engineering*, 129, 74-92, <http://dx.doi.org/10.1016/j.coastaleng.2017.09.005>

### SINBAD fixed bed experiment:

- van der A, D. A., van der Zanden, J., O'Donoghue, T., Hurther, D., Cáceres, I., McLelland, S. J., & Ribberink, J. S. (2017). Large-scale laboratory study of breaking wave hydrodynamics over a fixed bar. *Journal of Geophysical Research: Oceans*, 122(4), 3287-3310. <http://dx.doi.org/10.1002/2016jc012072>.
- van der Zanden, J., van der A, D. A., Cáceres, I., Hurther, D., McLelland, S. J., Ribberink, J. S. & O'Donoghue, T. (2018). Near-bed turbulent kinetic energy budget under a large-scale plunging breaking wave. *Journal of Geophysical Research: Oceans*, 123(2), 1429-1456. <http://dx.doi.org/10.1002/2017jc013411>
- SINBAD fixed bed dataset, 4TU data repository, <https://data.4tu.nl/repository/uuid:753f1d84-36e5-47fa-b74b-55c288545b9b>

### Numerical studies related to SINBAD experiments

- Zheng, P., Li, M., Van der A, D. A., van der Zanden, J., Wolf, J., Chen, X., & Wang, C. (2017). A 3D Unstructured Grid Nearshore Hydrodynamic Model Based on the Vortex Force Formalism. *Ocean Modelling*, 116, 48-69. <http://dx.doi.org/10.1016/j.ocemod.2017.06.003>
- Fernandez-Mora, A., Ribberink, J. S., van der Zanden, J., van der Werf, J. J., & Jacobsen, N. G. (2016). RANS-VOF modeling of hydrodynamics and sand transport under full-scale non-breaking and breaking waves. 35th Conference on Coastal Engineering, Antalya, Turkey. <http://dx.doi.org/10.9753/icce.v35.sediment.29>



## Appendix A

*Overview of experimental runs: cross-shore location front (i.e. sea-ward side) measurement frame , time interval within experiment (corresponding to bed profile development).*

Run	$x$ (m)	$t$ interval (min)		Run	$x$ (m)	$t$ interval (min)
1	51.0	0-15		37	56.0	0-15
2	51.0	15-30		38	56.0	15-30
3	51.0	30-45		39	56.0	30-45
4	51.0	45-60		40	56.0	45-60
5	51.0	60-75		41	56.0	60-75
6	51.0	75-90		42	56.0	75-90
7	60.0	0-15		43	58.0	0-15
8	60.0	15-30		44	58.0	15-30
9	60.0	30-45		45	58.0	30-45
10	60.0	45-60		46	58.0	45-60
11	60.0	60-75		47	58.0	60-75
12	60.0	75-90		48	58.0	75-90
13	55.5	0-15		49	56.5	0-15
14	55.5	15-30		50	56.5	15-30
15	55.5	30-45		51	56.5	30-45
16	55.5	45-60		52	56.5	45-60
17	55.5	60-75		53	56.5	60-75
18	55.5	75-90		54	56.5	75-90
19	57.0	0-15		55	63.0	0-15
20	57.0	15-30		56	63.0	15-30
21	57.0	30-45		57	63.0	30-45
22	57.0	45-60		58	63.0	45-60
23	57.0	60-75		59	63.0	60-75
24	57.0	75-90		60	63.0	75-90
25	54.5	0-15		61	55.0	0-15
26	54.5	15-30		62	55.0	15-30
27	54.5	30-45		63	55.0	30-45
28	54.5	45-60		64	55.0	45-60
29	54.5	60-75		65	55.0	60-75
30	54.5	75-90		66	55.0	75-90
31	59.0	0-15		67	53.0	0-15
32	59.0	15-30		68	53.0	15-30
33	59.0	30-45		69	53.0	30-45
34	59.0	45-60		70	53.0	45-60
35	59.0	60-75		71	53.0	60-75
36	59.0	75-90		72	53.0	75-90